Simulation of the Spread of *Phytophthora cinnamomi* Causing a Root Rot of Fraser Fir in Nursery Beds

K. M. Reynolds, H. J. Gold, R. I. Bruck, D. M. Benson, and C. Lee Campbell

First author, former graduate research assistant, Department of Plant Pathology, North Carolina State University, Raleigh 27695-7616; second author, professor and director, Biomathematics Program, Department of Statistics, North Carolina State University; third, fourth, and fifth authors, associate professor, professor, and associate professor, respectively, Department of Plant Pathology, Raleigh. Present address of first author is Department of Plant Pathology, Ohio Agricultural Research and Development Center, Wooster 44691.

This research was supported in part by a grant from the North Carolina Christmas Tree Growers Association.

Journal Series Paper 9634 of the North Carolina Agricultural Research Service, Raleigh 27695-7601.

Portion of Ph.D. thesis submitted by the first author to North Carolina State University.

The use of trade names in this publication does not imply endorsement by the North Carolina Agricultural Research Service of the products named, nor criticism of similar ones not mentioned.

We wish to thank J. H. van der Vaart and R. Silber for assistance with some of the algorithms developed for the simulation program.

Accepted for publication 30 December 1985 (submitted for electronic processing).

ABSTRACT

Reynolds, K. M., Gold, H. J., Bruck, R. I., Benson, D. M., and Campbell, C. L. 1986. Simulation of the spread of *Phytophthora cinnamomi* causing a root rot of Fraser fir in nursery beds. Phytopathology 76:1190-1201.

A model was developed to simulate the spread of *Phytophthora cinnamomi* in Fraser fir in nursery beds. The major system submodels were seedling growth and pathogen spread. The submodels for seedling growth described root and shoot development. Regression models described seedling height as a function of degree-days and shoot dry weight as a function of seedling height and degree-days. Regression models also related shoot dry weight to seedling root attributes. The submodel for pathogen spread described root colonization as a function of soil temperature, interseedling infection across root contacts or small interroot distances, and pathogen spread when soil moisture is suitable for zoospore movement and infectivity. Results of validation studies demonstrated good agreement between the model and portions of field data. Discrepancies were most pronounced in late summer. Alterations in system parameters associated with unusually dry soil conditions in late summer significantly improved agreement between the model and field data. Model response was insensitive both to changes in soil saturation period and to the functional relationship between inoculum efficiency and interroot distance. Parameters whose variation caused weak or inconsistent effects are rhizosphere width in flooded or nonflooded soil and colonization rate of the pathogen along the roots. In contrast, variations in interseedling distance, time of season, probability of interseedling infection by hyphal growth, and chlamydospore production elicited strong and consistent model responses.

Systems analysis and computer simulation have been widely applied in the fields of plant and animal ecology (10,25,26). Botanical epidemiology is a specialization within population ecology and, as such, the benefits of a systems approach are similarly available (12). In particular, systems analysis provides a paradigm for addressing complex modeling problems effectively and efficiently (15).

A number of plant disease simulators have been published since Waggoner and Horsfall (25) first published EPIDEM (5). Bloomberg's (2) simulation model for damping-off caused in Douglas-fir (*Pseudotsuga menziesii* (Mirb.) Franco) seedlings by *Fusarium oxysporum* Schlect. was the first simulation model for a soilborne fungal pathogen. Secondary infection processes were not included in the Douglas fir/Fusarium model, because secondary infection was inconsequential (2). Gilligan (10) recently reviewed the status of root disease modeling and noted that this field is still in its infancy because of the complexities entailed in studying soilborne disease in any detail.

The objective of the present study was to develop a disease simulator for the spread of *Phytophthora cinnamomi* Rands in Fraser fir (*Abies fraseri* (Pursh) Poir.) in nursery beds. The simulator is intended as a research tool for use in evaluating the influence of various site, host, pathogen, and environmental factors on the initiation and spread of disease.

The model for spread of *P. cinnamomi* consists of a submodel for growth of 2-yr-old Fraser fir seedlings and a submodel for pathogen activity. Both submodels are composed of input/output relations based on regression models (11). System couplings that interrelate host and pathogen activity are based on previous work (18,20,21) and general biological knowledge of the system. Three aspects of system structure that involve couplings between the host and pathogen submodels are fungal colonization of Fraser fir roots, infection across root contacts by mycelial growth, and infection involving zoospore movement.

General descriptions of the submodels for host growth and pathogen activity are presented in appropriate subsections of the Materials and Methods section. The definitions of the principal system variables are presented in Table 1. Specific relations among model variables (equations 1–15) are presented in the Results section. Assumptions concerning system behavior are introduced at appropriate points of discussion in the latter section and are summarized in Table 2. Detailed descriptions of algorithms for model implementation on a computer are presented by Reynolds (18).

MATERIALS AND METHODS

Development of model for seedling growth. Seedling growth consists of submodels for bud flush in the spring, increase in shoot height (H), increase in shoot dry weight (S), and root structural development (Fig. 1). A submodel for fungal colonization couples the seedling growth submodel and the pathogen submodel (Fig. 1). We assumed that soil moisture was not a limiting factor for seedling growth in an irrigated nursery (Table 2) and that, consequently, the progress of spring bud flush, as well as subsequent H and S increments could be predicted as functions of cumulative degree-days (Fig. 1). Spatial structure of seedling root systems is completely specified by defining a root's depth of origin on the taproot, its length, and orientation in the horizontal and vertical planes. The total number of primary roots as well as their total length are determined by regression functions (7).

The publication costs of this article were defrayed in part by page charge payment. This article must therefore be hereby marked "*advertisement*" in accordance with 18 U.S.C. § 1734 solely to indicate this fact.

Experiments with Fraser fir were conducted with 2-yr-old seedlings obtained from the Linville River Nursery in Crossnore, NC. Two-year-old seedlings were used because root systems of younger seedlings were too restricted for secondary spread of inoculum via root contact, and root systems of older seedlings were too complex for analysis.

Mean hourly soil and air temperatures were recorded with thermistors (model UUT51J1; Fenwal Electronics, Framingham, MA) attached to a model CR-21 Micrologger (Campbell Scientific Inc., Logan, UT). The air-temperature thermistor was located 30 cm above the nursery bed in an insulated, reflective housing that was aspirated by a battery-driven fan that pulled air across the sensor at a rate of approximately 2 m/sec (6). Soil temperature thermistors were located at depths of 5 and 19 cm within one of the blocks in the nursery beds. Soil matric potential at a depth of 5 and 19 cm was monitored with Bouyoucos gypsum blocks (model CEL-WFD; Beckman Instruments, Fullerton, CA) attached to the micrologger. However, calibration of the gypsum blocks in the laboratory indicated that moisture data were too unreliable for use as a data input to the simulator. For that reason, the moisture data were used only to establish approximate soil moisture conditions during validation studies.

The progress of seedling bud flush (B) was monitored in a random sample of 180 Fraser fir seedlings from 1 May 1983 to 10 June 1983. The proportion of flushed seedlings was recorded at 2- and 3-day intervals.

Increase in H was monitored in 50 randomly selected seedlings. For each seedling, H was recorded at 2-wk intervals from 15 May 1983 to 12 August 1983. An additional 50 seedlings were selected at random at each sampling date for destructive sampling and their heights were recorded. Seedlings from the destructive sampling were then oven dried at 85 C for 48 hr and weighed.

Several attributes of root system structure related to S were studied from 15 May to 9 August 1981. Random samples of 50 seedlings were taken at 2-wk intervals. Seedlings were excavated hydraulically with a backpack-type, hand-pump sprayer. Shoots were severed at the root crown, oven dried at 85 C for 48 hr, and weighed. Root systems were mapped on a Tektronix digitizing board connected to a Tektronix 4051 graphics terminal (Tektronix Corp., Portland, OR). Roots were stored in moist soil at 15 C until analyzed. Taproot length, the position of attachment of each primary root in terms of depth relative to the root crown, and the length of each root were recorded for each seedling. Secondary roots were so infrequent on 2-yr-old seedlings that data were not collected. A data summarization program was written to calculate and summarize taproot length (R_1), total primary root length (R_2), and total primary root number (R_3), the distribution of the proportion of total primary root length (P), and number (Q, Table 1) along the taproot in depth increments equal to one-tenth of the taproot length for each seedling.

The seedling growth model was originally composed of strictly deterministic relations. Simulations of seedling growth were conducted to provide partial verification of this submodel. Seedling heights before bud flush in 1983 were used to initialize H in a simulated population of 25 seedlings. Population variances and covariances for S, R_1, R_2, and R_3, in the simulated population of seedlings were compared with the corresponding sample estimates from the 1981 data. Population variances and covariances for the four variables were much smaller than the corresponding sample estimates. Therefore, stochastic effects were

TABLE 1. Summary of model variables used in simulation of the spread of *Phytophthora cinnamomi* in 2-yr-old Fraser fir seedlings in nursery beds

Variable name	Description	Used in equations:	Variable name	Description	Used in equations:
α, λ	Parameters of Beta-probability density used to characterize dependence of root vertical angle distribution on depth of root origin on tap root	9a, 9b, 9c	Q_K	Proportion of primary roots of a seedling in the K_{th} depth increment	8
			R_1	Taproot length (mm) of a seedling	4
a	Shape parameters controlling steepness of function defining propagule efficiency as a function of propagule-to-root distance	13	R_2	Total primary root length (mm) of a seedling	5
			R'_2	Normally distributed stochastic parameter that determines rate of conversion of S to R_2 (mm/mg)	5
B	Probability of seedling bud flush	1			
C_c	Cumulative degree-days (reference date is 1 April; (reference temperature is 0 C)	1, 2, 3	R_3	Total primary root number of a seedling	6
			R'_3	Normally distributed stochastic parameter that determines rate of conversion of S to R_3	6
C_i	Daily degree-day increment	2			
D	Distance (mm)	13	S	Seedling shoot dry weight (mg)	3, 4, 5, 6
E	Absolute propagule efficiency (infections per propagule; depends only on propagule-to-root distance)	13, 14c	S'	Normally distributed stochastic parameter that determines rate of shoot dry weight accumulation of a seedling (mg per mm*degree-day)	3
e	Experimentally determined efficiency, which depends on soil saturation period (infections per propagule)	14 a	T	Soil temperature (C)	10
			t	Time (days)	2, 12
			t_2	Time (hr)	14a, 14b
e_a	Actual propagule efficiency, which depends on propagule to root distance and duration of a soil saturation event (infections per propagule)	14c, 15	W	Rhizosphere width (mm) of a seedling	11
			w_1	Minimum rhizosphere width (mm) of a seedling when soil is not saturated but soil matric potential is above field capacity	...
e_p	Relative (or proportional) efficiency, which is scaled from a minimum of 0 to a maximum of 1	14b, 14c			
			w_2	Maximum rhizosphere width (mm) when soil is saturated	...
F_1	Rate of root colonization (mm per day)	10			
F_2	Chlamydospores produced per mm of root	12	X	Binomially distributed random variable (number of successful infections received on a root that is neighboring an infected root)	15
H	Height of 2-yr-old seedlings (mm)	2, 3			
H'	Normally distributed stochastic parameter that modifies rate increase height of 2-yr-old seedlings	2	X_1	Class variable in MANOVA model (22) indicating data type (field or model data) in validation experiments	0
K	Index to depth increments along the tap root of a seedling (1, 2, ..., 10)	7, 8	X_2	Class variable in MANOVA model (22) indicating seedling block (A, B, C, or D) in validation experiments	0
M	Soil matric potential (millibars)	11			
m	Percentage of soil moisture	12			
n	Number of chlamydospores on an infected root segment that are available to initiate infection on a neighboring root	15	X_3	Class variable in MANOVA model (22) indicating plot (1, 2, . . ., 10) in validation experiments	0
			X_4	Interaction term in MANOVA model (22), (X_1 by X_2)	0
P	Proportion of total root length colonized by *P. cinnamomi*		X_5	Interaction term in MANOVA model (22), (X_1 by X_3)	0
P_K	Proportion of primary root length of a seedling in the K_{th} depth increment	7			

introduced into the relations involving H, S, R_2, and R_3, by assuming that a rate or shape parameter in each relation (H', S', R'_2, and R'_3, respectively) was a normally distributed random variable (3,6) (Table 2). A stochastic process was used to assign a specific parameter value to each seedling at initialization of simulation on the assumption that a unique relation between submodel variables is characteristic for each seedling (Table 2). The parameters H', S', R'_2, and R'_3, have a mean equal to the regression estimate of the parameter and variance determined by trial and error to produce acceptable agreement. The variance of R_1 and its covariance with S, R_1, and R_3 in the simulated population agreed well with the 1981 data after a stochastic effect was introduced into the relation for H and S, because R_1 depends on H and S.

Description of submodel for pathogen activity. Data on several aspects of pathogen behavior that are presented in this study are summarized from previous work (13–15). The conceptual model for pathogen activity (Fig. 10) illustrates three basic pathways by which spread could occur.

Mean hourly soil temperature data for soil depth intervals of 4–6 and 18–20 cm were input to the simulation program. Mean hourly soil temperatures for all other soil depth intervals were obtained by linear interpolation because the nursery beds were covered by shade frames to reduce the amount of direct solar radiation reaching the soil surface (K. Cassel, *personal communication*). The hourly temperature data for each 2-cm soil depth interval were used to compute hourly rates of lesion extension at each depth. Both the proximal and distal limits of a lesion were incremented once per day by the sum of the hourly increments. Because the endpoints of lesion extension of any given lesion may lie in different depth intervals, the proximal and distal rates of lesion extension may differ. The simulator allows two simultaneous, nonoverlapping infections to occur on a root at any given time (Table 2). If two adjacent lesions occupy the same segment of root, they were merged during the time step in which the overlap was first detected. If the simulator generated a third lesion on a root, the pair that lay in closest proximity to one another were merged in that time step. The limit of two simultaneous and distinct lesions on a root was not as restrictive as it might appear. The colonization rate of *P. cinnamomi* on Fraser fir roots was so high (equation 10) that the occurrence of more than two such lesions was a rare event. The rarity of the latter three lesions partially depends on the relatively low occurrence of root associations with a potential for spread of the pathogen. In addition, when zoospores initiate infection, only a single lesion is generated on a successfully infected root in the model (Table 2). However, more than one root may be infected by zoospores from a single infected root.

As colonization of an infected seedling by *P. cinnamomi* progresses, the possibility of spread to neighboring seedlings by one of three pathways is enhanced (Fig. 10). Spread between neighboring seedlings may be accomplished by hyphal growth if an uninfected (target) root is either touching an infected (source) root or within some minimum distance (w_1) from the source root.

Only two soil moisture conditions were distinguished in simulation for simplicity, including flooded (0 mbar matric potential) or some constant negative potential (Table 2). The simulation model requires the input of two rhizosphere widths corresponding to these conditions; maximum width, w_2, for flooded and minimum width, w_1, for nonflooded. Mycelial spread of the pathogen from an infected root was presumed to occur with

TABLE 2. Summary of model assumptions used in simulation of the spread of *Phytophthora cinnamomi* in 2-yr-old Fraser fir seedlings in nursery beds

1.	Stochastic parameters (R'_1, R'_2, and R'_3) used to predict root structural attributes (R'_1, R'_2, and R'_3, respectively) are normally distributed random variables (6).
2.	Parameters, R'_1, R'_2, and R'_3, are asigned to each seedling at initialization of simulation and are characteristic of an individual's root growth behavior.
3.	A nonlinear relation exists between the proportion of functional root loss and shoot dry weight accumulation of a seedling (Fig. 3). Root loss is measured as length of root that is colonized or distal to a lesion, because absorptive roots were observed to be uniformly distributed along a seedling's primary roots (K. M. Reynolds, *unpublished*).
4.	Azimuthal angle of root orientation is distributed uniformly over the interval $[0,2\pi]$; vertical angle of root orientation is distributed as a Beta-probability function whose parameters are functions of a root's depth of origin on the taproot (equations 9a–c).
5.	Two simultaneous, nonoverlapping lesions are allowed on a root at any given time. Overlapping lesions are merged into a single lesion.
6.	A single lesion is generated on a root that is successfully infected by inoculum associated with an infected root.
7.	In nonsaturated soil near field capacity, a root can become infected by inoculum from a neighboring infected root if the two roots are within a distance, w_1. The source of inoculum is assumed to be chlamydospores on the surface of the infected root (13,17,20). A probability of infection, TMIN, is associated with the infection event. TMIN is assumed to be 1 when the soil matric potential is greater than or equal to field capacity.
8.	In saturated soil, a root can become infected by inoculum from a neighboring infected root that lies within a distance, w_2. The source of inoculum is assumed to be chlamydospores (on the surface of an infected root) that have germinated to produce sporangia that liberate zoospores (13,20,21).
9.	Inoculum in soil occurs in the form of chlamydospores associated with infected root fragments. These fragments are assumed to be uniform about the x, y, and z axes.
10.	Rate of root colonization depends only on soil temperature when soil matric potential is greater than or equal to field capacity.
11.	Soil matric potential is maintained at or above field capacity in the nursery environment when regular irrigation schedules are followed.

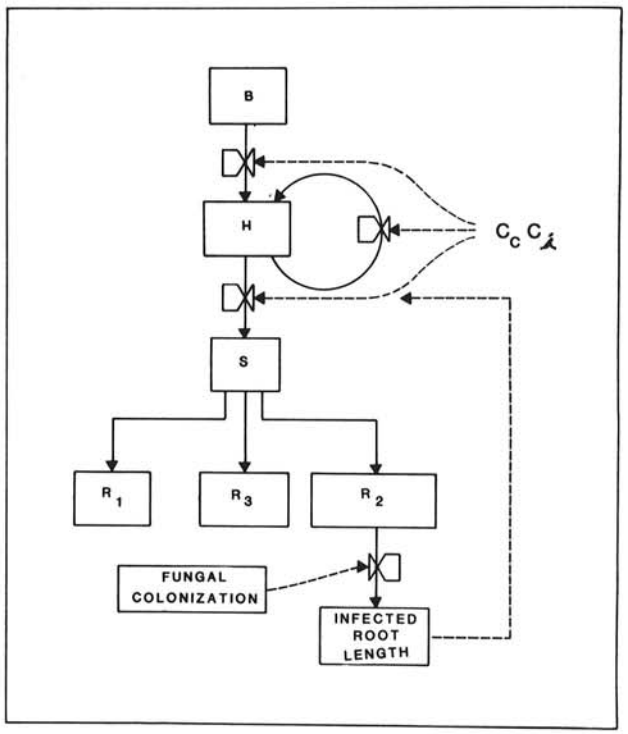

Fig. 1. Conceptual model of Fraser fir seedling growth. Cumulative degree-days (C_c), determine the probability of seedling bud flush (B) in the spring (equation 1, in text). Seedling shoot elongation was initiated at bud flush, and was calculated as a function of C_c, C_i, and the seedling's most recently calculated height (H; equation 2, in text). Increase in shoot dry weight (S) was calculated as a function of C_c and H, and was adjusted by the proportion of nonfunctional root length in the previous time step. At the end of each time step, the total length of infected root on each seedling was calculated by summing individual lesion lengths. Root attributes (R_1, R_2, and R_3), are calculated as functions of S (equations 4, 5, and 6, respectively).

probability, TMIN (model input), whenever a neighboring root was within the minimum distance, w_1, of the infected root.

We assumed that, under soil moisture conditions that do not allow zoospore movement (13), infection by mycelia was accomplished by germinating chlamydospores at or near the root surface (20), because mycelium that would have given rise to this form of inoculum is not persistent in moist soil (17) (Table 2). We further assumed that chlamydospore inoculum was always associated with roots, although inoculum was not restricted to living roots. Inoculum in soil was assumed to be associated with root fragments (Table 2). When inoculum in soil was specified in the model, input values for the number of root fragments, mean fragment length, and the standard deviation of length was supplied. Stochastic processes were used at model initialization to distribute the root fragments uniformly throughout the soil volume. Fragment length was assigned, assuming a normal distribution, and fragment orientation in space was specified, assuming uniform angular distributions about the x, y, and z axes. As a consequence, inoculum in soil was assumed to be clustered, because it was associated with root fragments, but the clusters were assumed to be uniformly distributed (Table 2).

An algorithm (18) was developed to determine if an arbitrary pair of roots was within the minimum or maximum rhizosphere width (w_1 or w_2, respectively). The source root was represented geometrically by a cylinder with a maximum infective radius of w_2 (model input) and a minimum infective radius of w_1 (model input), whereas the potential target root was represented by a line (18). The equations for source and target root constituted a pair of simultaneous equations. The algorithm solved for the determinant of the associated Jacobian matrix of coefficients. If the target root intercepted, or was capable of intercepting at some future point in time, the infective cylinder of a source root, then the distance of closest approach of the target root to the source root was calculated by computing the minimum distance between the two roots at the midpoint of each 1-mm segment of source root within the segment of infective cylinder traversed by the target root or its projection (18). Infection was considered to have occurred as soon as the target root was long enough to reach the source root if the distance of closest approach was less than or equal to w_1 (18).

Infection also occurred by zoospore movement, which may involve the production of sporangia either from the mycelium of the pathogen associated with infected root tissue or from chlamydospores produced on or within infected root tissue. Previous work indicated that the former source of sporangia was probably inconsequential (20).

The rhizosphere was considered to expand to a radius of w_2 during saturated soil conditions (Table 2); both the date of a saturation event and the duration of the event were system inputs. If a saturation event occurred, the infection algorithm was used to check all root pairs previously identified as potential cases of pathogen transmission, to determine whether a potential target root was currently within the infective radius of a source root (18). The length of infected root tissue within a distance w_2 of the segment of target root traversing the infective cylinder was computed if the target root was within the range, w_2, at which zoospore infection could occur (18). Infection by zoospore inoculum was then treated as a stochastic process that employed a binomial distribution to determine infection probability for the calculated number of chlamydospores that were available to initiate infection.

Model validation. Data on spread of *P. cinnamomi* among 2-yr-old Fraser fir seedlings in nursery beds at the Linville River Nursery in 1983 were compared with predicted values generated by the model. No data pertaining to model development were taken from the plots used in model validation. Four blocks (designated A, B, C, and D), each consisting of 48 plots, were carefully thinned to five seedlings per plot including a central seedling in May 1983. Most of the root system of the rogued seedlings was removed to minimize the potential for pathogen colonization of senescing root fragments. Plot size in blocks A, B, C, and D was 20, 25, 25, and 30 cm on a side, respectively. Plot size was selected to reduce the risk of interplot interference due to root growth between neighboring plots and was based on studies in 1981 of root structural development.

Inoculum segments were prepared by flooding a tub containing 50 3-yr-old Fraser fir seedlings with a zoospore suspension of *P. cinnamomi* (20) and harvesting the infected roots after 18 days. The central seedling in each plot was inoculated by positioning four 1-cm-long segments of infected root next to the taproot at 2-wk intervals starting with block A on 13 June, block B on 27 June, block C on 11 July, and block D on 25 July. At the time of inoculation, seedling height within a block was recorded. Distance and direction for each seedling within a plot relative to the inoculated seedling were recorded. The 48 plots within a block comprised four groups of 12 plots. Seedlings in each group were harvested at weekly intervals after inoculation. Groups 1, 2, and 3 were exposed to ambient soil moisture. In group 4, seedlings were flooded 2 wk after inoculation and harvested after an additional week. The plot was flooded by driving four steel plates ($1 \times 45 \times 90$ cm) 10–15 cm deep to form a rectangular enclosure (group 4). Water was initially applied to the surface and then to trenches lining the inner walls of the enclosure at 15-min intervals for 4 hr to maintain soil moisture close to saturation at the soil surface.

Seedlings were sealed in plastic bags at sampling and stored in an ice chest. Seedlings were cultured on a semiselective medium (23) within 24 hr. The cultures were assessed at 24 and 48 hr for seedling infection as evidenced by growth of *P. cinnamomi* on the culture plate. Data for group 3 of block C were not obtained; all seedlings in this group were severely damaged by unidentified insect larvae.

Model predictions and field data were summarized by group; for each group, the frequency of plots with an observed number of infected seedlings was recorded. Criteria for judging the degree of correspondence between the model and field data were: location of the mode of the distribution, height of the mode, and concentration about the mode. In addition, multivariate analysis of variance (MANOVA) and canonical correlation were used to assess quantitatively the degree of correspondence between the model and field data (22). The following model was specified in the MANOVA procedure:

$$Y = XB \tag{0}$$

Y is a 30×5 matrix whose row elements consist of the observed or predicted number of plots in a group exhibiting 0, 1, 2, 3, or 4 infected seedlings. X is a 30×5 matrix whose column elements are the predictors x_1, x_2, x_3, x_4, and x_5 as defined in Table 1. B is a 5×5 matrix of regression coefficients. The significance of all effects involving data source was tested by using the approximate F-statistic associated with Pillai's trace (22). Results from the canonical correlation analysis were assessed using criteria developed by Bartlett (1) and Cooley and Lohnes (4).

Sensitivity analysis. The most significant model variables were selected for evaluation. These were: interseedling distance, time of season, minimum rhizosphere width for pathogen spread by mycelial growth (w_1), rhizosphere width for infection by zoospores under flooded soil conditions (w_2), soil saturation period, a zoospore infection efficiency parameter, probability of infection by mycelial growth from an infected root (TMIN), colonization rate parameter, and a chlamydospore production parameter.

For each variable, three plots from blocks B and C were selected. Selection was based on the potential of a plot to show some degree of response, as judged by number of seedlings infected, to changes in the variable. For instance, a plot would not be selected if all seedlings had been infected in the field, and the lowest values of the parameter to be evaluated were close to the value expected in the field and increases in the value of the parameter were expected to result in increased infections. Ten simulations were run for each plot at each of three or four levels of the variable.

The influence of interseedling distance was evaluated by adding 0, 5, 10, or 20 mm to the original distances between the inoculated and surrounding seedlings, whereas the relative spatial relations of the group of five seedlings were kept constant.

The effect of time of season was evaluated by starting the simulation either on the actual date of inoculation (13 June, group

1 in block A) or 20 or 40 days later. At the start of simulation, seedling height was set the same as the field data so that seedling size was not a factor.

The infection efficiency parameter for zoospores (equation 13a) determines the slope of the function (equation 13). The colonization rate parameter and the chlamydospore production parameter define the proportion of fungal growth rate and chlamydospore production, respectively, and are used to rescale calculated values for equations 10 and 12, respectively.

RESULTS

Development of model for seedling growth. The first operation performed in simulation was initialization of seedling root structure before seedling bud flush in the spring. The reference temperature for degree-day summation was 0 C, whereas the reference date from which to sum degree-days was 1 April. The probability that an individual seedling will have buds that flushed by a given date is given by:

$$B = 1.0 - 1.056 \exp(-0.013(C_c - 303)) \quad (1)$$

Equation 1 accounted for 96% of experimental variation (Fig. 2) (F-test significant at $P = 0.0001$). An individual seedling was designated as flushed in the model if a uniform random deviate (Uniform [0,1]) was less than the probability of B. If the cumulative degree days (C_c) was less than 308 degree-days, there was no bud flush activity. If C_c was greater than 510 degree-days, any seedlings with buds not already flushed were "forced." A stochastic process was employed to determine if bud flush occurred on a particular date for all seedlings in the simulated population that had not already flushed when C_c was between 308 and 510 degree-days. At 510 degree-days, the calculated value for equation 1 was 0.93, and bud flush was forced to occur once 510 degree-days had accumulated because no functional form could be found that adequately described the entire process.

The variables H and S and root system structure are initialized before the time at which C_c could be expected to reach 308 degree-days. Once a seedling had buds that flushed, increase in H and S and root structural development were initiated (Fig. 1). Height increment data on individually identified seedlings had been collected at 2-wk intervals. Seedling heights on days between sampling dates were estimated for each seedling by linear interpolation to obtain a description for daily height increase. A model, obtained by stepwise regression analysis, was developed for the augmented height growth data, which accounted for 99% of the variation (F-test significant at $P = 0.0001$). Despite the very high R^2 value for the height growth model, long-term predictive ability was poor in simulation verification trials for seedling growth. Consequently, model parameters were adjusted so that predicted seasonal trends in the mean and standard deviation of height compared favorably with estimates obtained from the independent random samples of seedling height growth in the study involving destructive sampling. The revised height growth model ($R^2 = 0.75$) was:

$$H_{t+1} = 0.94 - 0.03\,C_i - 0.00026\,C_c + (H' + 0.002\,C_i - 0.00003\,C_i - 0.00009\,C_c + 0.00003\,C_c^2)\,H_t \quad (2)$$

with variables as defined in Table 1.

H' is normally distributed with mean 1.025 and variance 0.00001. S of a seedling at time t was a function of H at time t and C_c (Fig. 1). The model was obtained from the destructive sampling growth data. The resulting regression accounted for 87% of experimental variation (F-test significant at $P = 0.0001$) and is given by:

$$S = 31.49 - (0.05 - S'\,\mathrm{H})C_c \quad (3)$$

in which S' is a normal random deviate with mean 0.001958 and variance 0.00003. A stochastic process was used to assign values of S' to individual seedlings during initialization of simulation.

Change in S also was regulated in the model by the extent of fungal colonization of the root system (Fig. 1). Data on seedling growth response to extent of root colonization were not available, so a hypothetical relation between S increase and the proportion of functional root loss was specified (Fig. 3). The amount of root loss for each seedling was defined as the proportion of total root length that was colonized by the pathogen, including uncolonized but nonfunctional root tissue isolated from the shoot by the infection. We assumed that increases in S would depend on linear root loss, because of the almost uniform distribution of absorptive short roots on a Fraser fir primary root (Table 2)(Reynolds, *unpublished*). We further assumed that the relation between increase in S and linear root loss was nonlinear, because luxury production of root mass is a well-recognized phenomenon (Fig. 3, Table 2).

Regression models for the relation between S and R_1, R_2, and R_3 are summarized in equations 4, 5, and 6, respectively (also see Figs. 4–6):

$$R_1 = 26.62\,(S - 3.14) \quad (4)$$

$$R_2 = -73.54 + R'_2\,S \quad (5)$$

$$R_3 = 1.10\,(S - 17.59)\,R'_3 \quad (6)$$

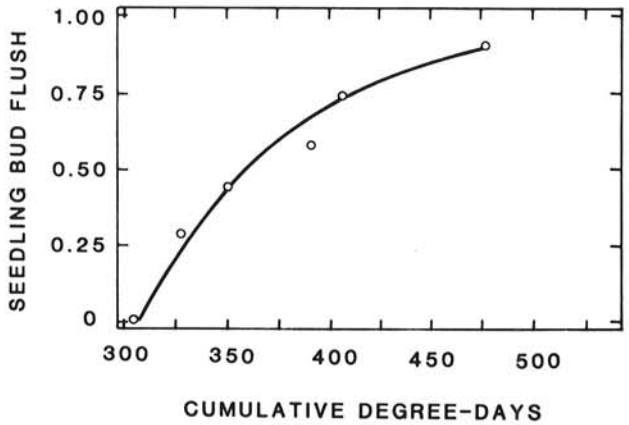

Fig. 2. Probability of bud flush (B) of 2-yr-old Fraser fir seedlings in the spring as a function of cumulative degree-days (C_c) Where: $B = 1.0 - 1.06 \exp[-0.01(C_c - 303)]$, $R^2 = 0.96$. The temperature baseline is 0 C, and the reference date is 1 April.

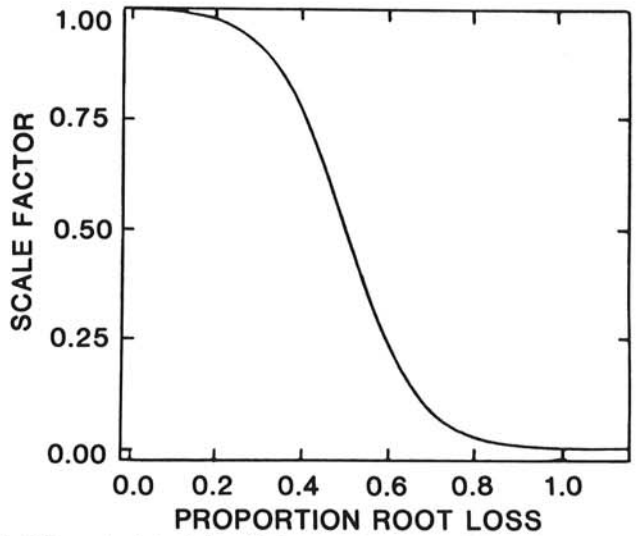

Fig. 3. Hypothetical relationship between shoot dry weight (S) increment of 2-yr-old Fraser fir seedlings and the proportion of functional root loss due to colonization by *Phytophthora cinnamomi* as given by the equation: $S = 1 - 1/1 + \exp[-12.0\,(P - 0.5)]$.

in which R'_2 and R'_3 are normally distributed stochastic parameters assigned to individual seedlings during initialization of seedling root structure:

$$R'_2 \sim N(5.61,0.0064)$$
$$R'_3 \sim N(0.66,0.0016).$$

Analyses of the distribution of primary root length and number along the taproot of a seedling (p and q, respectively) indicated that primary root length and number were independent of S and that the proportions of root length and number in a given depth class depended only on depth class (Figs. 7 and 8):

$$P_k = 37.52\,((K-0.5)^A\,(10.5-K)^{-0.08}) - 1.0 \qquad (7)$$

in which: $A = 0.54 - 0.96\,\log(K-0.5)$
and K = soil depth class (1,2,...,10)

$$Q_k = 14.58\,((K-0.5)^A\,(10.5-K)^{0.24}) - 1.0 \qquad (8)$$

in which: $A = 0.80 - 0.85\,\log(K-0.5)$ and K = soil depth class (1,2,...,10).

The R^2 values for equations 4–8 were 0.94, 0.92, 0.95, 0.91, and 0.89, respectively.

The spatial structure of the root system also must include the azimuthal and vertical angles of each root. Because these angles could not be calculated from digitized root data, subjective assessments were made by observation of root orientations when root systems were washed during sampling. The azimuthal angles of a sample of roots were assumed to be distributed uniformly over the interval $[0,2\pi]$ radians with the orientation of each root independent of the orientation of all other roots (Table 2). Although root vertical angle was variable, roots rarely were observed growing toward the soil surface from lower depths. In general, the mean downward angle was observed to increase with the depth at which a primary root originated on the taproot, and this agrees with observations of other coniferous species (2,20). A hypothetical model (Table 2) for variation in root vertical angle (VA) with depth is represented by a Beta-probability density function, which is defined in equations 9a–c (see also Fig. 9A and B):

$$\mathrm{VA} \sim \mathrm{beta}\,(\alpha, \lambda) \qquad (9a)$$

$$\alpha = 1 + 2/(1 + 10\exp(-0.1D)) \qquad (9b)$$

$$\lambda = 6 - \alpha \qquad (9c)$$

with variables as defined in Table 1. Since $\alpha + \lambda$ equals a constant (equation 9c), the concentration parameter of the distribution is assumed to remain constant with depth (3). The relationship between α and λ is illustrated in Figure 9B. The mode of the VA

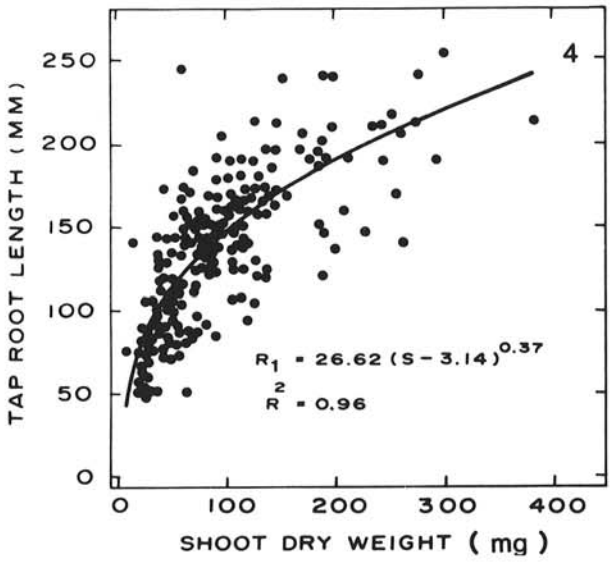

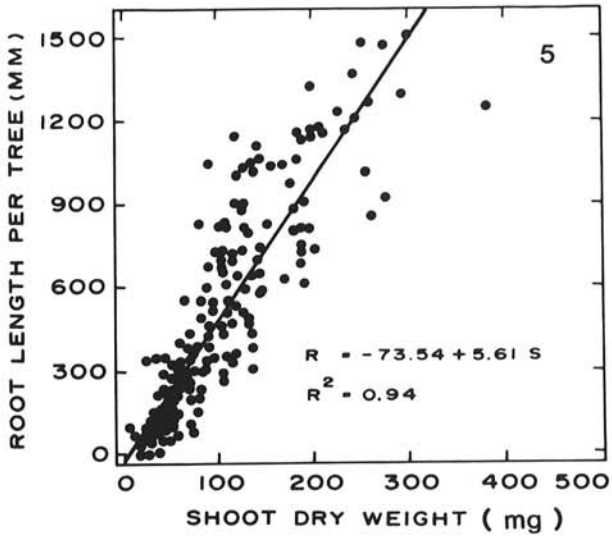

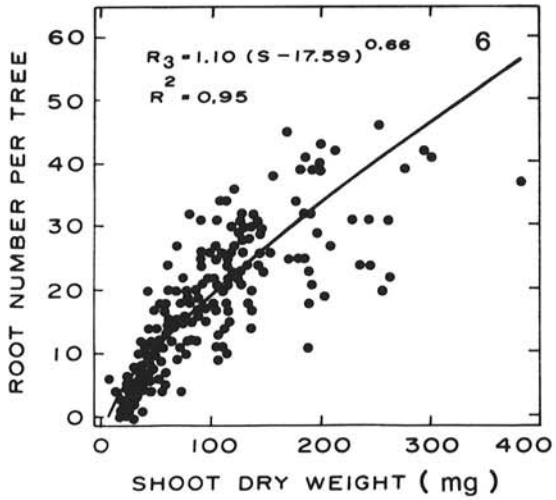

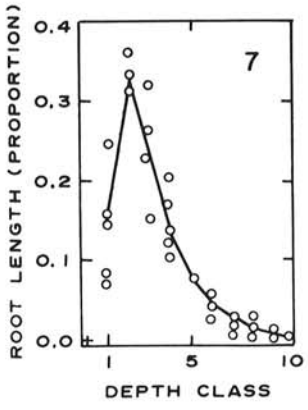

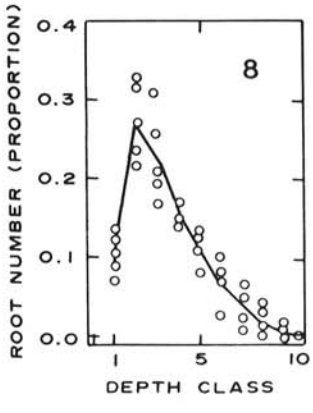

Figs. 4–8. Root structural attributes of 2-yr-old Fraser fir seedlings. Random samples of 50 seedlings were taken at 2-wk intervals from 15 May to 9 August 1981 from beds at the Linville River Nursery, Crossnore, NC. **4,** Relation between taproot length (R_1) and seedling shoot dry weight (S) (equation 4, in text). **5,** Relation between total primary root length (R_2) and S (equation 5, in text). **6,** Relation between total primary root number (R_3) and S (equation 6, in text). **7,** Distribution of the proportion of total primary root length (P) among 10 relative depth classes equal to one-tenth of the total taproot length (equation 7, in text). **8,** Distribution of the proportion of total primary root number (Q) among 10 relative depth classes equal to one-tenth of the total tap root length (equation 8, in text). Depth interval 1 is closest to the root crown.

distribution in response to soil depth shifted with depth (Fig. 9A).

Description of submodel for pathogen activity. Reynolds et al (20) obtained the following model for rate of Fraser fir root colonization by *P. cinnamomi* when soil moisture was not a limiting factor (Table 2):

$$F_1 = 0.008\,(T - 10^{2.70}(34 - T)^{1.21} \quad (10)$$

with variables as defined in Table 1.

Equation 10 accounted for 95% of experimental variation (*F*-test significant at $P = 0.0001$). Physical simulation of acropetal and basipetal root colonization (direction respective to a point of primary root attachment to the taproot) was conducted by using excised and unexcised roots. No differences in colonization rate were detected (21). For purposes of computer simulation, F_1 was divided by 24 to obtain estimates of hourly lesion extension.

Reynolds et al (21) obtained an expression for rhizosphere width of Fraser fir when the infective propagule was a chlamydospore of *P. cinnamomi* so that:

$$W = 4.01\,(1 - M)^{-0.72} \quad (11)$$

with variables defined in Table 1.

Equation 11 accounted for 82% of experimental variation (*F*-test significant at $P = 0.0001$) and predicts a rhizosphere width of 0.09–0.07 mm when M is within the range of −200 to −300 mbar. This range corresponds approximately to field capacity. Equation 11 is relatively insensitive to changes in M in the range indicated, so we assumed that a single value for rhizosphere width, applicable to nonsaturated soil conditions, could be specified (Table 2). Because seedlings were irrigated regularly in the nursery bed, M probably fluctuated within the above limits during summers that have a normal quantity and distribution of rainfall.

Reynolds et al (20) found that sporangium production by the vegetative thallus of *P. cinnamomi* was very limited on roots of 2-yr-old Fraser fir seedlings and was confined to the succulent, actively growing root tips. In contrast, large numbers of chlamydospores were recovered from nonsterile soil in which infected Fraser fir roots had been incubated for as few as 10 days (20). We assumed in the model that zoospores were produced from sporangia arising from germinating chlamydospores on the root surface or in the immediate soil environment (Table 2). Reynolds et al (20) obtained a model by stepwise regression analysis for chlamydospore production over time on roots incubated at different soil moistures:

$$F_2 = 0.004\,(24.11 + 7.47t - 0.16t^2)M \quad (12)$$

with variables as defined in Table 1.

Equation 12 accounted for 91% of the variation (*F*-test significant at $P = 0.0001$).

Under saturated soil conditions, chlamydospore density per unit length of root was then calculated with equation 12. Each chlamydospore has an infection efficiency, E, which is a function of the average minimum distance in mm, D, between the potential target and source roots:

$$E = 1/(1 + D^a) \quad (13)$$

in which a was a parameter supplied as a system input to determine the slope of the efficiency function (equation 13). The value of E calculated in equation 13 represents inoculum efficiency at a given distance under saturated soil conditions when time is not a limiting factor for zoospore movement. Reasonable estimates of the parameter, a, lie in the interval [1,3] based on comparisons between equation 13 and a surface response model for zoospore movement (18).

Saturation periods of 16 hr or more resulted in maximum infection efficiency (21). Reynolds et al (21) obtained an empirical

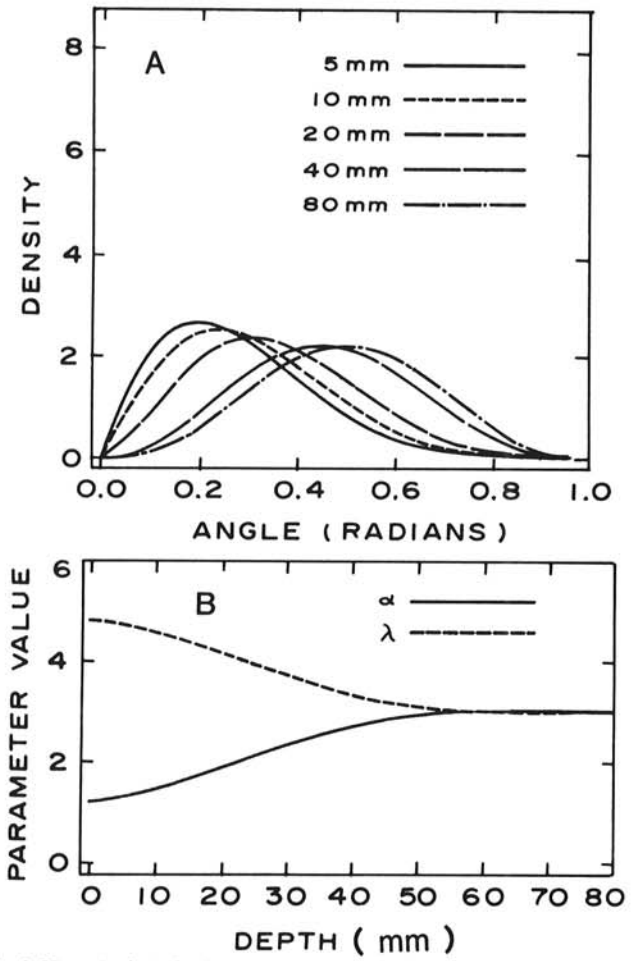

Fig. 9. Hypothetical distribution for root vertical angle, based on subjective assessments for vertical angle orientation of roots of Fraser fir seedlings that were hydraulically excavated from beds at the Linville River Nursery. Root vertical angle is described by equations 9a–c in text. **A,** Shift in the mode with increasing depth of origin of a root. **B,** Dependence of the parameters α and λ on depth of root origin (equations 9a and 9c, in text). Note that $\alpha + \lambda$ is constant, hence the concentration remains constant.

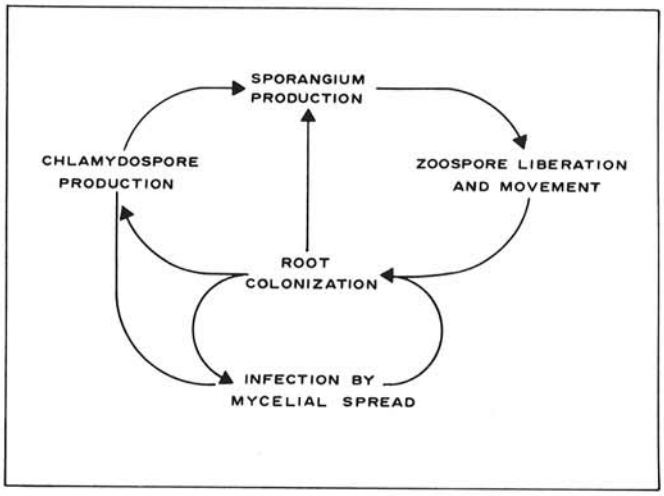

Fig. 10. Conceptual model of behavior of *Phytophthora cinnamomi* on Fraser fir roots. The rate of fungal colonization of 2-yr-old Fraser fir roots was temperature dependent (equation 10, in text). Interseedling spread of the pathogen by mycelial growth across root contacts or small interroot distances was assumed to occur whenever two roots (of the same or different seedings) were within a minimum distance, w_1, of each other. The length of infected root as well as the length of time the root has been infected determine the number of chlamydospores associated with an infected root segment (equation 12). During conditions of soil saturation, chlamydospores germinate and form sporangia that liberate zoospores, which can swim short distances and infect nearby roots.

model for infection efficiency as a function of saturation period when the duration was 16 hr; it is

$$e = 0.044\, t_2^{0.635} \quad (14a)$$

with variables as defined in Table 1.

Equation 14a accounted for 63% of experimental variation (F-test significant at $P = 0.0004$). Equation 14a was derived for the specific case of an assumed maximum efficiency, E, equal to 0.30. The fitted regression line, however, yields a value of $e = 0.26$. For purposes of simulation, equation 14a was rescaled to express e as a proportion, e_p, of maximum efficiency, E, where maximum efficiency was regarded as a variable quantity that depended on spore-to-root distance (eqution 13); e_p, then, was the proportion of E realized during a specific soil saturation event:

$$e_p = 0.172\, t_2^{0.635} \quad (14b)$$

The value 0.172 in equation 14b scales the equation so that e_p assumes values in the interval [0,1]. The actual efficiency, e_a, of a single chlamydospore is therefore:

$$e_a = e_p\, E \quad (14c)$$

The probability of infection for a population of chlamydospores follows the binomial distribution so the probability of obtaining at

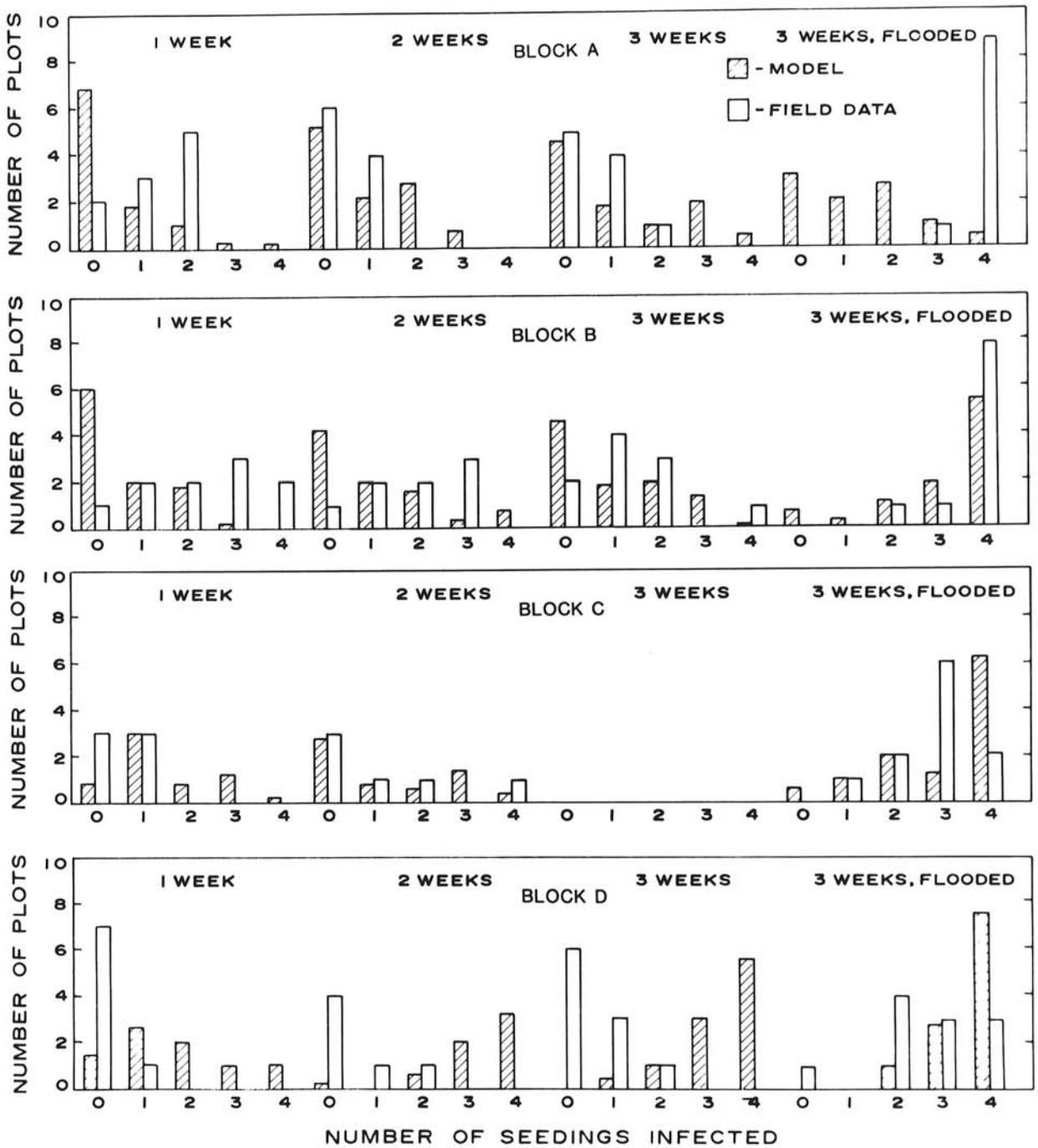

Fig. 11. Validation test results for spread of *Phytophthora cinnamomi* in blocks (A to D) of nursery bed of Fraser fir seedlings. Each block contained 48 plots of 2-yr-old Fraser fir seedlings. Blocks were sampled as described in the text. For all simulated plots, five iterations of the model were performed and the results averaged. System variables employed in all simulations were: $w_1 = 1.1$ mm, $w_2 = 5$ mm, and soil saturation period equaled 8 hr. All treatments experienced some loss in plots due either to lack of initial infection or seedling damage caused by root-feeding grubs. In all cases, the number of simulated plots per treatment corresponds to the number of field plots retained for analysis.

least one successful infection given n spores is given by:

$$P(x \geq 1) = 1 - (1-e_a)^n \quad (15)$$

with variables as defined in Table 1.

Infection was treated as a stochastic event in the model. The probability of infection (equation 15) was calculated and compared with a random number, Q, distributed as Uniform[0,1]. If $P(X \geq 1)$ was greater than Q, then infection occurred.

Model validation. The results of the MANOVA procedure demonstrate that neither model or field data (X_1) or interaction effects involving X_1 and block (X_4) or X_1 and group (X_5) were significant. For the three effects, the approximate F-statistics were $F(5,12) = 0.22$ (probability of greater $F = 0.95$), $F(15,42) = 1.29$ (probability of greater $F = 0.25$), and $F(15,42) = 0.47$ (probability of greater $F = 0.94$), respectively. The only effect involving data type (X_1) that was found to approach significance was the data type by block interaction (X_4 in equation 0; probability of greater $F = 0.25$). As discussed in the qualitative analysis of the data, below, discrepancies between the model and field data in block D of the validation experiments probably were the largest contributing factor to the latter result. The block effect approached significance [$F(15,42) = 1.28$; probability of greater $F = 0.26$], whereas the group effect was highly significant [$F(15,42) = 2.12$; probability of greater $F = 0.03$].

The canonical R^2, or the amount of redundancy observed in the model and field data, was 0.54 when the data for the first four roots were considered to provide nontrivial solutions (4). Using stricter criteria, however, only data for the first two roots were significant (1); with the latter criteria, the cumulative canonical R^2 was 0.35. As a compromise, we considered data for roots with a canonical correlation greater than 0.80 to be significant. In the latter case, the data for the first three roots were significant and had a cumulative canonical R^2 equal to 0.48.

In the validation trials (Fig. 11), all system inputs were held constant (saturation period = 8 hr, $w_1 = 1.1$ mm and $w_2 = 5$ mm). Good agreement between the model and the field data was obtained for groups 2 and 3 of block A, group 4 (flooded) of block B and group 2 of block C. When classes 0 and 1 for group 3 of block B and classes 3 and 4 for group 4 of block C were combined, distributions of infection frequency were very similar to the field data.

Comparisons for the remaining groups (Fig. 11) agreed poorly. With a few exceptions, reasonable justifications could be proposed to account for the discrepancies (Fig. 11). The distributions of infection frequency generated by the model were markedly skewed to the right for group 1 of blocks A and B (Fig. 11). Early in the growing season, seedling root systems were quite small and, therefore, it was likely that the four inoculum pieces exerted a disproportionately large influence on infection of root systems of neighboring, uninoculated seedlings relative to the influence of the root system of the inoculated seedling. This influence would, however, be expected to diminish with increasing seedling size.

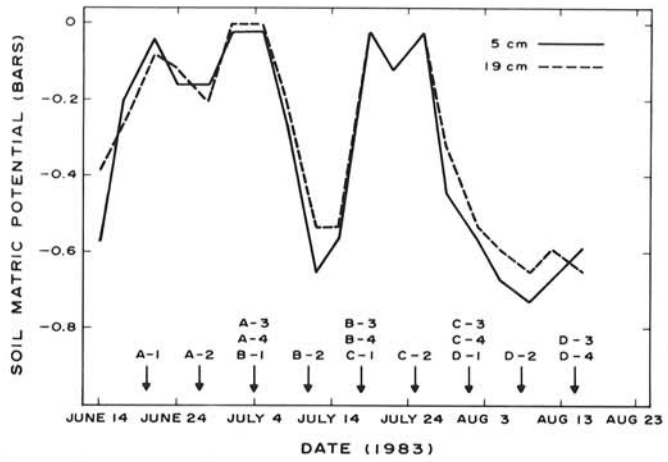

Fig. 12. Seasonal trend in soil matric potential in nursery beds of Fraser fir seedlings at the Linville River Nursery, Crossnore, NC. Moisture values presented within the figure are mean matric potentials from 0500 to 0600 hours. Arrows indicate sampling date(s).

A further discrepancy between the model and the field data pertains to the procedure used to flood experimental plots. The distribution of infected seedlings for group 4 (flooded) of block A is strongly skewed to the left compared with the predicted distribution (Fig. 11). As described earlier, care was taken to avoid surface ponding of water. In the first run (group 4, block A), however, the application method was not satisfactory and a certain amount of surface ponding did occur. Because zoospores of *Phytophthora* exhibit negative geotaxis (16) and movement is greatly enhanced in surface films of water compared with movement within the soil matrix (8), it appears likely that the high incidence of infection reported for group 4 of block A resulted from zoospore movement within water films on the soil surface. In the second run (group 4, block B), the flooding procedure was improved to minimize surface ponding and, in this case, the model and data were in good agreement (Fig. 11).

In general, good agreement between the model and field data was obtained for block C, whereas the model appeared to depart seriously from observed infection rates in block D (Fig. 11). The summer of 1983 was characterized by lower than average rainfall in the region, particularly in the latter half of the season. Contrary to expectations, regular nursery irrigation was not sufficient to keep up with evapotranspiration, resulting in a progressive reduction in soil matric potential (Fig. 12). In a typical year, however, rainfall is more or less evenly distributed over the summer.

Initially, we assumed that soil moisture did not limit colonization rate, mycelial infection, or chlamydospore production on roots (20). Because there is no reliable method for continuous and accurate recording of soil moisture, no provision was made to describe the effects of soil moisture on the types of fungal activity mentioned above. The model does, however, allow for changes in colonization rate, probability of pathogen spread by mycelial growth, chlamydospore production, and zoospore inoculum efficiency when suitable hypotheses can be put forward.

The unexpectedly low matric potentials observed in the latter part of the summer (Fig. 11) represent a departure from model assumptions (Table 2). Thus, we examined a posteriori effects of a drying soil on certain aspects of model behavior in an attempt to explain the lack of agreement between the model and field data. However, in doing so, it should be recognized that such a procedure does not represent a validation of the model.

For better agreement between the model and the field data, we introduced the assumption for blocks C and D that the progressive drying of the soil resulted in a reduced minimum rhizosphere width so that pathogen spread by mycelial growth could occur only if roots were in actual physical contact ($w_1 = 0.9$ mm). It also proved necessary to assume, in the case of block D, that the probability of this event was minimal (TMIN = 0.10). Implementation of these assumptions in the model had little effect on results with block C, but resulted in close agreement between the model and field data for block D (Fig. 13).

The assumption of a drastic reduction in the probability of pathogen spread by mycelial growth (TMIN = 0.10) for block D is based on the assumption that the dry soil conditions induced hardening off of the roots, rendering them less susceptible to infection. Concurrent, less extreme reductions in TMIN, w_1 and the root colonization rate also may improve agreement between the model and field data. Detailed studies of each of the latter effects would be valuable for further elucidation of the dynamics of spread of *Phytophthora* spp. As our field data indicate (Figs. 11 and 13), significant spread of *P. cinnamomi* in Fraser fir can occur in the absence of saturated soil conditions. Marx and Bryan (14) also reported pathogen spread by mycelial growth under dry soil conditions. Weste et al (27) described patterns of disease extension in Australian forests, which also indicate spread by mycelial growth across root contacts. A clearer understanding of the influence of soil moisture on processes other than zoospore movement would be useful.

Sensitivity analysis. Little change was observed in the predicted number of infected seedlings for saturation periods of 2, 4, 8, and 16 hr and for zoospore infection efficiency parameter values of 1, 2, and 3. All other system variables had some influence on the number of seedlings infected. The lack of significant effect of the zoospore infection efficiency parameter, a, on simulated seedling infection was unexpected, because predicted efficiency is relatively sensitive to changes in the value of a. For instance: at 2 mm, efficiency was predicted to be 0.33, 0.20, and 0.11 when a (equation 13) was 1, 2, and 3, respectively. The lack of sensitivity to changes in a may have been because mycelial spread was relatively common in the plots selected. More extensive sensitivity tests on parameter a are required to determine its sensitivity both in the presence and absence of frequent instances of spread by mycelium in order to identify conditions under which the model may be sensitive to changes in the value of a.

The lack of response in seedling infection to changes in soil saturation period also was unexpected and may be rationalized as a consequence of two interacting factors. First, inoculum efficiency (equation 14) does not drop off rapidly in response to reduced saturation period. At 2 hr, for instance, the probability of infection was still predicted to be approximately 25% of maximum; second, a large number of chlamydospores were available to initiate new root infections whenever any portion of a target root falls within the infective cylinder of an infected root. In effect, there was a surplus of chlamydospore inoculum over a short term that effectively compensated for significant reductions in the infective ability of a single propagule. Furthermore, the rate of colonization was so rapid that most 2-yr-old seedlings were completely colonized within 1 wk of initial infection so that a large number of infected roots thus became available.

Model variables that strongly and consistently influence the number of infected seedlings were: interseedling distance (Fig. 14A), time of season (Fig. 14B), probability of pathogen transmission by mycelial growth (Fig. 14E), and the chlamydospore production parameter. The values assigned to w_1 (Fig. 14C), w_2 (Fig. 14D), and the colonization rate parameter (Fig. 14F) had some effect on seedling infection, but these effects are more variable both with respect to strength of the response and consistency between plots.

This division of variables into two sets, one showing strong and consistent effects and the other not as obvious, may indicate how much other variables not considered in a specific sensitivity analysis could modify the effect of the variable under consideration. For example, with the colonization rate parameter (Fig. 14F), the inoculated seedling in plot 2 was relatively closer to the four other seedlings compared with seedlings of plots 1 and 3, and greater spread by mycelial growth was predicted for plot 2 than for plots 1 or 3. Consequently, given a greater number of avenues by which infection could occur, colonization rate of the seedling root system had a significant influence.

DISCUSSION

The model presented for *P. cinnamomi* deals with secondary spread of a fungal pathogen and is the first of its kind to include a root pathogen with a relatively complex behavior. A number of assumptions were made to complete the specification of model structure (Table 2). The model was significantly limited in two respects: It deals only with 2-yr-old Fraser fir seedlings, and it does not deal explicitly with the effects of soil moisture status on colonization rate, pathogen spread by mycelial growth, or chlamydospore production.

The first limitation was a practical one; the model completely specifies the spatial organization of the root system of a seedling and evaluates root proximities and pathogen spread potential on a root-by-root basis. Although such a procedure was practical for very small plants with simple root structure, it is impractical when applied to larger plants with complex root structure. The method was warranted, however, for intensive studies of pathogen

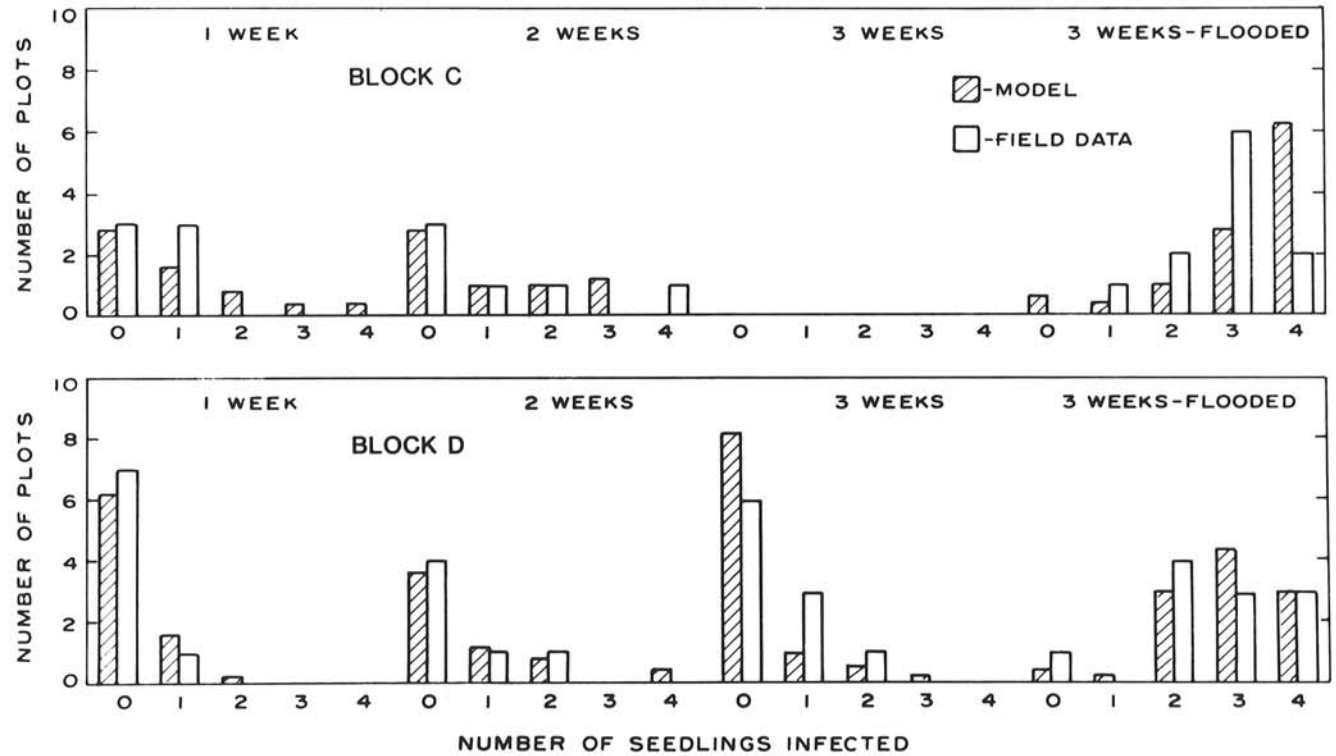

Fig. 13. Test results for spread of *Phytophthora cinnamomi* in nursery blocks C and D of Fraser fir seedlings when TMIN = 0.10. Alternative assumptions were made with respect to values of selected system inputs such as TMIN (the probability of pathogen spread by mycelial growth when roots are either touching or at least in close proximity), w_1 and duration of the soil saturation period in order to determine if alternative hypotheses about the system would improve agreement between field and model data. It was assumed for blocks C and D that soil moisture conditions prevailing in the latter part of the summer were sufficiently dry that pathogen spread by mycelial growth between seedlings could only be accomplished when roots were in physical contact. It was further assumed for block D that the probability of disease transmission across root contacts (TMIN) was 0.10. For both blocks C and D the saturation period was also reduced to 4 hr.

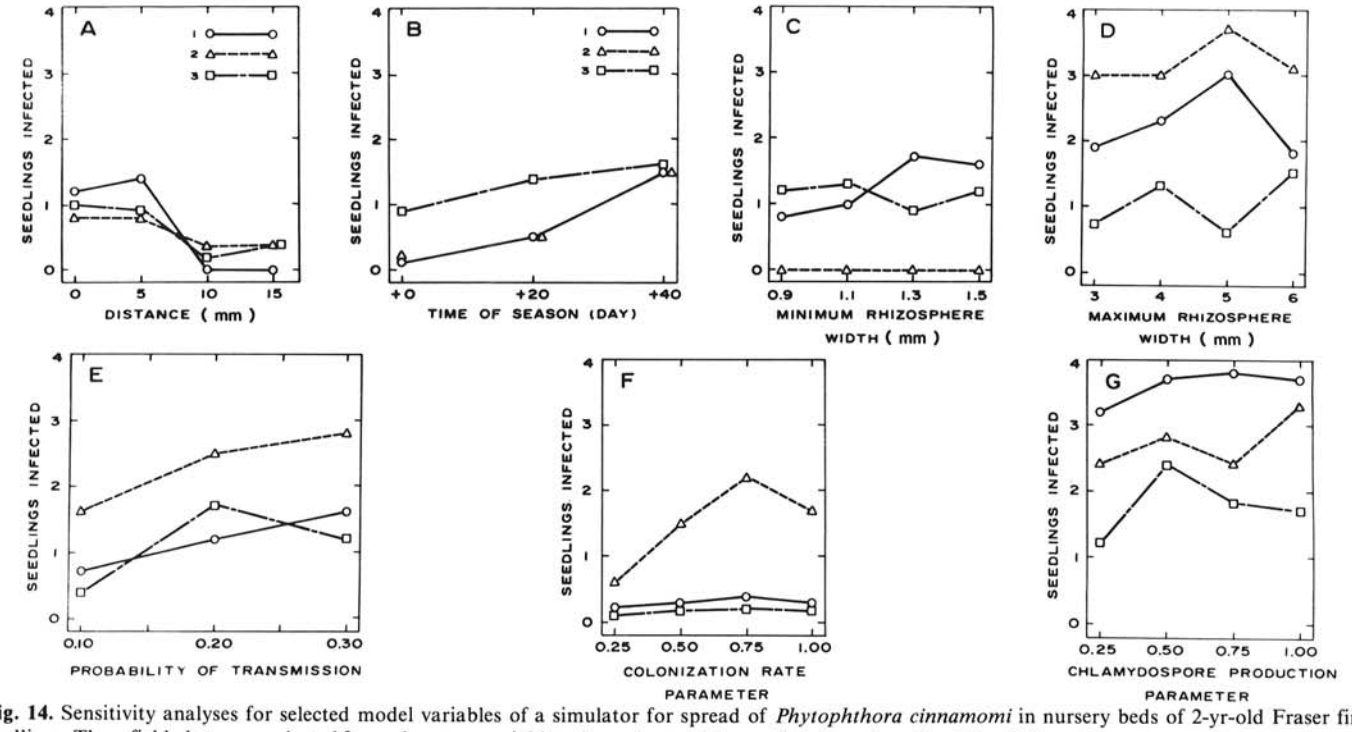

Fig. 14. Sensitivity analyses for selected model variables of a simulator for spread of *Phytophthora cinnamomi* in nursery beds of 2-yr-old Fraser fir seedlings. Three field plots were selected for each system variable to be evaluated. The predicted number of seedlings infected in response to varying levels of the variables represents the mean value of 10 iterations per plot. **A,** Effect of interseedling distance. *B,* Effect of time of season. Time of season refers to the time (in days after 1 April) at which simulation of infection was initiated. Time 0 in figure is 13 June, time 20 is 3 July, and time 40 is 23 July. **C,** Effect of minimum rhizosphere width (w_1). w_1 is the rhizosphere width under nonsaturated soil conditions. **D,** Effect of maximum rhizosphere width (w_2). w_2 is the rhizosphere width under saturated soil conditions. **E,** Effect of probability of pathogen spread by mycelial growth (TMIN). It is hypothesized that soil conditions may become sufficiently dry so that infection by mycelial growth from an infected root is less than certain even though a root may be within the minimum distance (w_1) of an infected root generally required for transmission of disease. **F,** Effect of the colonization rate parameter. The colonization rate parameter specifies a proportion of the colonization rate at which the fungus progresses along any given root (equation 10). *G,* Effect of the chlamydospore production parameter. The chlamydospore production parameter specifies a proportion of spore production on an infected root (equation 12).

movement. Model systems such as the one used in the present study may provide information on root disease dynamics that would not otherwise be obtainable, but probabilistic models of plant root density will generally be required. For such cases, the probabilistic model for determining root contacts developed by Thomson (24) will be of great value. Reynolds and Bloomberg (19) also have presented empirical models for calculating root contact frequency and developed discriminant models to predict the probability of contact frequencies for second-growth Douglas-fir stands.

The second major limitation of the model, lack of detailed information on soil moisture effects, arises because of the present inability to monitor soil moisture continuously with sufficient accuracy. This clearly limits the development of models for diseases induced by water molds because soil moisture is so critical (8,9). It is also a problem in modeling diseases caused by soilborne organisms in general. As discussed above, soil moisture status may influence both the colonization rate of a pathogen and the probability of root infection resulting from mycelial growth.

The validation studies demonstrated that the simulator performs well provided that critical model assumptions are not violated. In particular, the simulator performs poorly when soil dries appreciably below field capacity. Models for change in rhizosphere width (21) and chlamydospore production (20) in response to changes in soil moisture status could be incorporated into the simulator, but soil moisture must be accurately monitored to do so. Other aspects of pathogen activity also may be affected by dry soil conditions. Changes in the ability of the pathogen hyphae to cause infection may occur. In addition, the rate of root colonization may be affected by dry soil conditions. Both of the latter aspects of the behavior of *P. cinnamomi* need to be addressed more critically.

The sensitivity analyses demonstrated that interseedling distance, time of season, chlamydospore production, and the probability of infection by mycelial spread have a strong and consistent influence on infection incidence. Each of these results have important implications for management of diseases caused by *P. cinnamomi*. Because spread of the pathogen does not require conditions conducive to zoospore production and movement, nursery bed seedling density will generally influence the rate of spread. The analysis of time-of-season effect removed the influence of initial seedling size. It was observed, however, that infection incidence increased later in the season, an effect that probably resulted from faster seedling growth later in the season. Thus, larger seedlings in more densely planted beds may further increase the rate of pathogen spread.

The effect of soil moisture on the probability of spread by mycelial growth is hypothetical, whereas the effect on chlamydospore production has been demonstrated (20). Management practices that maintain soil moisture at a level that is sufficiently low may restrict fungal development and infection without adversely affecting seedling growth.

The sensitivity analysis also indicated that changes in the values of w_1, w_2, and the colonization rate parameter had weak and/or inconsistent effects on changes in infection incidence, whereas changes in the saturation period and zoospore infection efficiency parameter had almost no effect. We have noted, with respect to the first set of variables, that other variables not considered in a particular analysis may have influenced the results. This is equally true for the saturation period and zoospore infection efficiency parameter. More extensive sensitivity tests on all these variables are required to determine whether the model is generally insensitive to changes in the values of these variables or model sensitivity is conditional on the state of the system. In either case, experimental confirmation may provide useful additional insights into the dynamics of pathogen spread within this system.

LITERATURE CITED

1. Bartlett, M. S. 1941. The statistical significance of canonical correlations. Biometrika 32:29-38.

2. Bloomberg, W. J. 1979. Model simulations of infection of Douglas-fir seedlings by *Fusarium oxysporum*. Phytopathology 69:1072-1077.
3. Brunk, H. D. 1975. An Introduction to Mathematical Statistics. Xerox College Publishing, Toronto, Canada. 457 pp.
4. Cooley, W. W., and Lohnes, P. R. 1971. Multivariate Data Analysis. John Wiley & Sons, New York. 364 pp.
5. Cowling, E. B., and Horsfall, J. G. 1978. Prologue: How disease develops in populations. Pages 1-16 in: Plant Disease: An Advanced Treatise. Vol. II. How Disease Develops in Populations. J. G. Horsfall and E. B. Cowling, eds. Academic Press, New York. 436 pp.
6. Davis, J. M., Bruck, R. I., Runion, G. B., and Mowry, F. L. 1983. An aspiration system for meteorological sensors used in epidemiological studies. Phytopathology 73:1246-1249.
7. Draper, N. R., and Smith, H. 1966. Applied Regression Analysis. John Wiley & Sons, New York. 407 pp.
8. Duniway, J. M. 1976. Movement of zoospores of *Phytophthora cryptogea* in soils of various textures and matric potentials. Phytopathology 66:877-882.
9. Duniway, J. M. 1979. Water relations of water molds. Annu. Rev. Phytopathol. 17:431-460.
10. Gilligan, C. A. 1983. Modeling of soilborne pathogens. Annu. Rev. Phytopathol. 21:45-64.
11. Hall, C. A. S., and Day, J. W. Jr., eds. 1977. Ecosystem Modeling in Theory and Practice. John Wiley & Sons, New York. 684 pp.
12. Kranz, J., and Hau, B. 1980. Systems analysis in epidemiology. Annu. Rev. Phytopathol. 18:67-83.
13. MacDonald, J. D., and Duniway, J. M. 1978. Influence of the matric and osmotic components of water potential on zoospore discharge in *Phytophthora*. Phytopathology 68:751-757.
14. Marx, D. H., and Bryan, W. C. 1969. Effect of soil bacteria on the mode of infection of pine roots by *Phytophthora cinnamomi*. Phytopathology 59:614-619.
15. Overton, W. S. 1977. A strategy of model construction. Pages 49-74 in: Ecosystem Modeling in Theory and Practice. C. A. S. Hall and J. W. Day, Jr., eds. John Wiley & Sons, New York. 684 pp.
16. Pfender, W. F., Hine, R. B., and Stanghellini, M. E. 1977. Production of sporangia and release of zoospores by *Phytophthora megasperma* in soil. Phytopathology 67:657-663.
17. Reeves, R. J. 1975. Behaviour of *Phytophthora cinnamomi* Rands in different soils and water regimes. Soil Biol. Biochem. 7:19-24.
18. Reynolds, K. M. 1984. The epidemiology of Phytophthora root rot of Fraser fir. Ph.D. dissertation. North Carolina State University, Raleigh. 216 pp.
19. Reynolds, K. M., and Bloomberg, W. J. 1982. Estimating the probability of intertree root contact in second-growth Douglas-fir. Can. J. For. Res. 12:493-498.
20. Reynolds, K. M., Benson, D. M., and Bruck, R. I. 1985. The epidemiology of Phytophthora root rot of Fraser fir: Root colonization and inoculum production. Phytopathology 75:1004-1009.
21. Reynolds, K. M., Benson, D. M., and Bruck, R.I. 1985. The epidemiology of Phytophthora root rot of Fraser fir: Rhizosphere width and inoculum efficiency. Phytopathology 75:1010-1014.
22. SAS Institute 1982. SAS User's Guide. 1982 Edition. SAS Institute Inc., Cary, NC. 923 pp.
23. Shew, H. D., and Benson, D. M. 1982. Qualitative and quantitative soil assays for *Phytophthora cinnamomi*. Phytopathology 72:1029-1032.
24. Thomson, A. J. 1979. Derivation of root contact probability. For. Sci. 25:206-212.
25. Waggoner, P. E., and Horsfall, J. G. 1969. EPIDEM: A simulator of plant disease written for a computer. Conn. Agric. Exp. Stn. Bull. 698:1-80.
26. Watt, K. F., ed. 1966. Systems Analysis in Ecology. Academic Press, New York. 276 pp.
27. Weste, G., Ruppin, P., and Vithanage, K. 1976. *Phytophthora cinnamomi* in the Brisbane Ranges: Patterns of disease extension. Aust. J. Bot. 24:201-208.